Available online at www.sciencedirect.com
SCIENCE DIRECT®
Cryogenics 46 (2006) 262–272
Cryogenics
www.elsevier.com/locate/cryogenics

# Safety oriented analysis of cold helium–air mixture formation and stratification

Maciej Chorowski [a,*], Gabriela Konopka-Cupiał [a], Germana Riddone [b]

[a] Wroclaw University of Technology, Faculty of Mechanical and Power Engineering, Wybrzeze Wyspianskiego 27, 50-370 Wroclaw, Poland
[b] European Organization for Nuclear Research CERN, 1211 Geneva 23, Switzerland

Received 11 March 2005; received in revised form 15 November 2005; accepted 25 November 2005

**Abstract**

Cryogenic installations of superconducting accelerators contain significant amount of high density helium, mostly filling the cryostats and headers located in underground tunnels and caverns. In the case of emergency relief of the helium, oxygen deficiency hazard arises. The paper proposes a description of helium–air mixture formation based on turbulent jet physics. A condition of stratified flow onset is given resulting from dimensional analysis. A performed experiment of cold helium discharge to an instrumented test tunnel enabled identification of different stratified flow types together with corresponding measurements of oxygen concentration and temperature drop. The results can be used for safety analysis of oxygen deficiency hazard in confined areas, especially in the tunnels.


*Keywords:* Helium vapour (B); Oxygen (B); Gas mixtures (B); Flow visualization (D)

## 1. Introduction

Superconducting accelerators like Large Hadron Collider presently under construction at CERN may contain up to hundred tons of high density helium, liquid or supercritical, mostly filling the magnet cryostats and transfer lines located underground. Even though the LHC accelerator is characterised by high reliability, the performed risk analysis showed that some failures leading to the helium discharge to environment atmosphere cannot be excluded [1]. The instantaneous helium mass flow rates to the LHC tunnel can reach the value of several kg/s and the discharge pressure can be of the order of several bar. Helium discharge to the atmosphere can create physiological hazards like cold damage to living tissue and asphyxiation. The symptoms of oxygen deficiency are given in Table 1 [2]. Oxygen concentration drop below the safe level of 18% can decrease a man ability to perform tasks and may induce early symptoms in persons with heart, lung or circulatory problems. Oxygen concentration as low as 4% causes coma in 40 s, then convulsions, respiration ceases and death. Furthermore, due to low helium density, the oxygen deficient mixture can stratify and propagate along the tunnel eventually accumulating in the upper parts of pits and caverns. To avoid danger of personnel asphyxiation an understanding of helium–air mixture formation, its potential stratification and further propagation along the underground tunnel is necessary.

Oxygen content depletion is a result of mixing the discharged helium with the atmospheric air. The resulting oxygen concentration can be calculated on the assumption of homogenous mixture formation in the whole volume of the confined space [3], or it can be assumed that the relieved helium creates immediately a separated layer in the upper part of the tunnel or other space confinement, with practically zero oxygen content [4]. The homogenous mixing can be a case in laboratory rooms or experimental halls with good ventilation, while in the accelerator tunnels, a separation of buoyant helium rich layer would be expected.

Numerous safety oriented helium relief experiments, which were performed in different laboratories [4–13], have

* Corresponding author. Tel.: +48 71 320 23 25; fax: +48 71 320 42 28.
*E-mail address:* maciej.chorowski@pwr.wroc.pl (M. Chorowski).

0011-2275/$ - see front matter © 2006 Elsevier Ltd. All rights reserved.
doi:10.1016/j.cryogenics.2005.11.019

**Nomenclature**

*Symbols*

| | |
|---|---|
| $A$ | jet cross-section area |
| $Ar$ | Archimedes number |
| $Ba$ | Bakke number |
| $c_p$ | specific heat |
| $D$ | tunnel diameter |
| $D_o$ | helium outlet nozzle diameter |
| $F_b$ | buoyancy force |
| $F_i$ | inertia force |
| $F_v$ | viscosity force |
| $g$ | acceleration of gravity |
| $h$ | distance from the tunnel ground |
| $m$ | mass |
| $n$ | volume fraction |
| $p$ | pressure |
| $q_m$ | mass flow rate |
| $r$ | mass fraction |
| $R$ | gas constant |
| $Re$ | Reynolds number |
| $T$ | temperature |
| $u$ | velocity |
| $x$ | distance from the jet outlet |
| $\alpha$ | jet angle |
| $\rho$ | density |
| $\Delta\rho$ | density difference between air and helium–air mixture |
| $v$ | viscosity |

*Indexes*

| | |
|---|---|
| mix | mixture |
| $x$ | at the distance $x$ |
| $i$ | mixture component |
| $n$ | number of mixture components |
| air | air |
| $O_2$ | oxygen |
| min | minimum |
| He | helium |

Table 1
Symptoms of oxygen deficiency [2]

| $O_2$ concentration[a] at atmospheric pressure (%) | At-rest symptoms |
|---|---|
| 21–18 | No symptoms |
| 18–15 | Decreased ability to perform tasks; may include early symptoms in person with heart, lung or circulatory problems |
| 15–12 | Respiration deeper, pulse faster, poor coordination |
| 12–10 | Giddiness, poor judgment, lips slightly blue |
| 10–8 | Nausea, vomiting, unconsciousness, ashen face, fainting, mental failure |
| 8–6 | Death in 8 min; after 6 min 50% die and 50% recover with treatment, 100% recover with treatment in 4–5 min |
| 4 | Coma in 40 s; convulsion, respiration ceases, death |

[a] Concentration as a percentage volume fraction.

shown that the stratification of oxygen deficient layer is observed, however the oxygen content in the layer does not result either from the full mixing of the helium with the incoming air, or from the immediate pure helium separation, laying somewhere in-between the values resulting from two approaches. The experiments covered the specific cases and the applicability of the results was limited.

The analysis presented in this paper is oriented towards Oxygen Deficiency Hazard (ODH) estimation, and addresses the following issues:

- identification and description of the mixing mechanism properly describing the resulting air–helium mixture parameters and allowing the estimation of the maximum depletion of oxygen content in the atmosphere as a result of helium relief,
- location of oxygen deficient mixture, its potential separation, stratification and propagation along the tunnel.

## 2. Helium discharge into the atmosphere and formation of helium–air mixture

An emergency discharge of cryogens into the atmosphere usually takes the form of free turbulent jet as shown in Fig. 1. Free turbulent jet is characterized by high intensity of air entrainment to the discharged cryogen, it conserves the momentum along the axis and the angle of its cone can be determined only experimentally [14]. The helium and nitrogen turbulent jet angle has been experimentally estimated to be of $\alpha \approx 13°$ [15].

A one-dimensional equation of momentum conservation along the jet axis is given by Eq. (1).

$$\frac{d(\rho_{mix\_x} u_{mix\_x} A_x)}{dx} = 0 \quad \text{where } A_x = \pi x^2 tg^2 \alpha \tag{1}$$

Jet air entrainment can be calculated from the geometrical increase of the jet cross-section along the axis, taking into account the thermal expansion of cold helium resulting from the mixing with warm air [16]. Helium–air mixture density, temperature and the oxygen concentration can be calculated from Eqs. (2) to (8) derived from the ideal gas model applied to the mixture. The mixing process has been assumed to be isobaric.

The ideal gas model assumption results from weak intermolecular forces characteristic for helium, and low critical temperature of helium (5.2 K). The changes in the

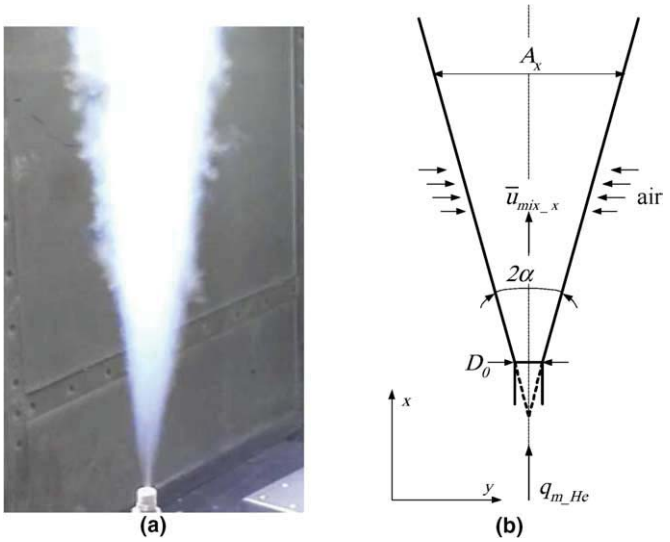


Fig. 1. Free turbulent jet: (a) photo of the cold helium jet; (b) jet geometric scheme.

temperature along the axis are the consequence of the warm air entrainment only. Heat conduction and radiation can be neglected.

$$\rho_{\mathrm{mix}\_x} = \frac{p_{\mathrm{mix}\_x}}{R_{\mathrm{mix}\_x} \cdot T_{\mathrm{mix}\_x}} \tag{2}$$

$$R_{\mathrm{mix}\_x} = \sum_i r_{i\_x} \cdot R_{i\_x} \tag{3}$$

$$r_{i\_x} = \frac{m_{i\_x}}{m_{\mathrm{mix}\_x}} = \frac{m_{i\_x}}{\sum_i m_{i\_x}} \tag{4}$$

$$T_{\mathrm{mix}\_x} = \frac{\sum_{i=1}^{n} m_{i\_x} \cdot c_{p,i\_x} \cdot T_{i\_x}}{m_{\mathrm{mix}\_x} \cdot c_{p,\mathrm{mix}\_x}} = \frac{\sum_{i=1}^{n} r_{i\_x} \cdot c_{p,i\_x} \cdot T_{i\_x}}{c_{p,\mathrm{mix}_{i\_x}}} \tag{5}$$

$$c_{p,\mathrm{mix}\_x} = \sum_i r_{i\_x} c_{p,i\_x} \tag{6}$$

$$r_{\mathrm{O}_2\_x} = \frac{0.21 \cdot m_{\mathrm{air}\_x}}{m_{\mathrm{mix}\_x}} \tag{7}$$

$$n_{\mathrm{O}_2\_x} = r_{\mathrm{O}_2\_x} \left( \frac{\rho_{\mathrm{mix}\_x}}{\rho_{\mathrm{O}_2\_x}} \right)_{p, T_{\mathrm{mix}\_x}} \tag{8}$$

The calculated helium–air mixture oxygen concentration, temperature and density are presented in Figs. 2–4. The results are obtained for the nozzle diameter equal to 0.01 m and the discharged helium pressure of 0.25 MPa. Regardless of the helium temperature $T_{\mathrm{He}\_0}$ at the relief point, the mixture oxygen content and the temperature are always increasing along the jet axis. The mixture density behaves according to the initial helium temperature.

If the discharged helium temperature is below 45 K, the mixture density initially decreases, reaches a minimum value ($\rho_{\mathrm{mix}} = \rho_{\mathrm{mix\_min}}$) lower than the density of air ($\rho_{\mathrm{mix}} = \rho_{\mathrm{air}}$) and then approaches again the air density (compare Fig. 4b). In spite of the helium initial high density, a warm air entrainment enables therefore the mixture stratification in the upper part of a confined space. When the discharged helium temperature is above 45 K, even though the outlet helium density is lower than the density

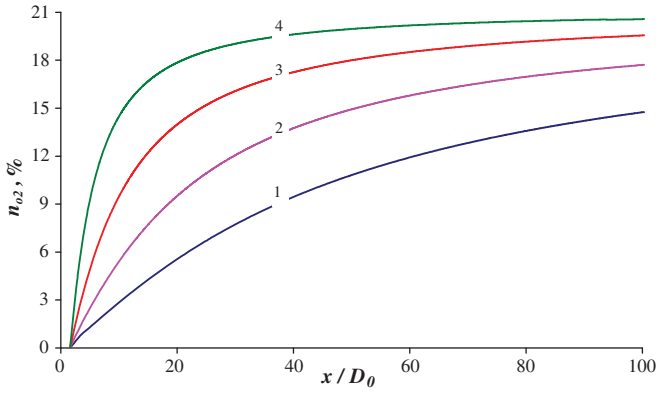


Fig. 2. Oxygen concentration in the mixture versus reduced distance from the jet outlet, where (1) $T_{\mathrm{He}\_0} = 10$ K, (2) $T_{\mathrm{He}\_0} = 25$ K, (3) $T_{\mathrm{He}\_0} = 50$ K, (4) $T_{\mathrm{He}\_0} = 100$ K.

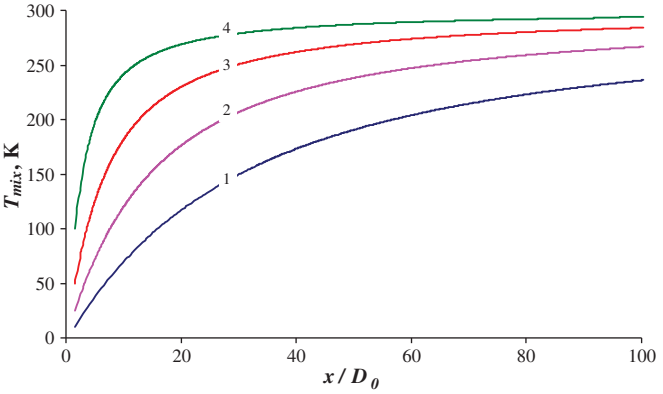


Fig. 3. Mixture temperature versus reduced distance from the jet outlet, where (1) $T_{\mathrm{He}\_0} = 10$ K, (2) $T_{\mathrm{He}\_0} = 25$ K, (3) $T_{\mathrm{He}\_0} = 50$ K, (4) $T_{\mathrm{He}\_0} = 100$ K.

of air it is still possible that there appears a minimum on the plot. This takes place for outlet helium temperature from within the range 45–55 K (compare Fig. 4c). For temperatures above 55 K the mixture density monotonically increases along the jet axis, towards the density of the air.

From the description of helium–air mixture formation based on the turbulent jet mechanism it follows that in the case of a cold helium discharge, the potentially stratified buoyant layer will always contain some amount of oxygen, resulting from the air entrainment. In a confined space (e.g. accelerator tunnel) the distance allowable for the jet formation is limited—compare Fig. 5. In case of the buoyant layer stratification, this distance must be long enough to let the mixture and air density at least equalize ($\rho_{\mathrm{mix}} = \rho_{\mathrm{air}}$).

## 3. Stratification of helium–air mixture

We conclude from the performed simulations that due to the entrainment of warm air, even for a very low initial helium temperature, the helium–air mixture density will

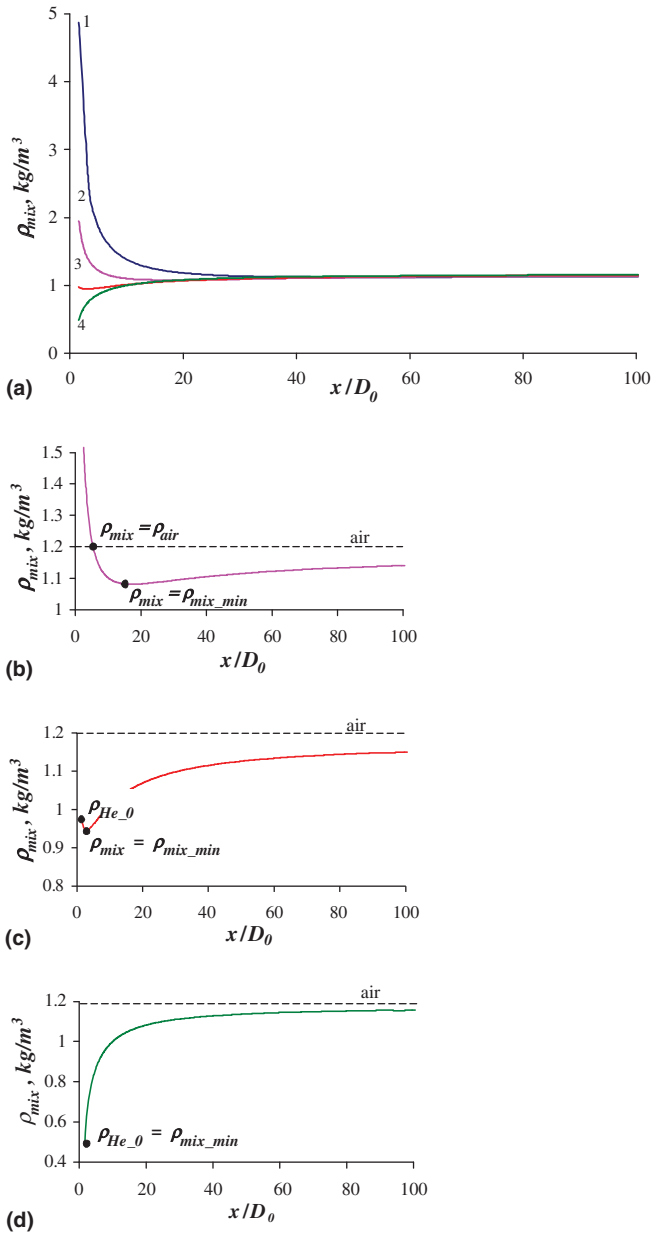


Fig. 4. Density of the mixture versus reduced distance from the jet outlet, where (a) (1) $T_{He\_0} = 10$ K, (2) $T_{He\_0} = 25$ K, (3) $T_{He\_0} = 50$ K, (4) $T_{He\_0} = 100$ K; (b) zoom of (2) $T_{He\_0} = 25$ K; (c) zoom of (3) $T_{He\_0} = 50$ K; (d) zoom of (4) $T_{He\_0} = 100$ K.

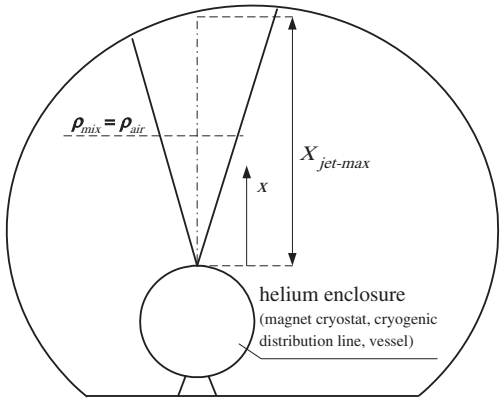


Fig. 5. Jet scheme in a tunnel.

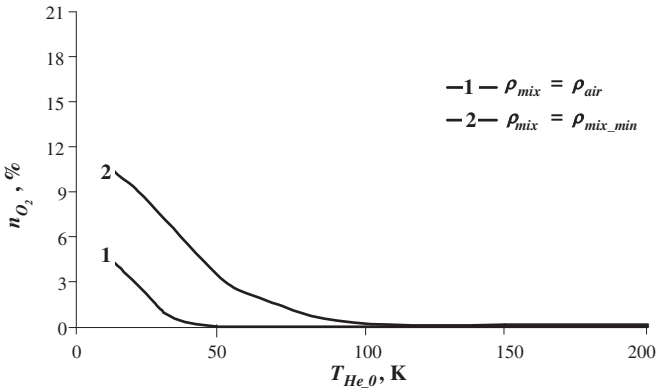

Fig. 6. Oxygen concentration in the buoyant region.

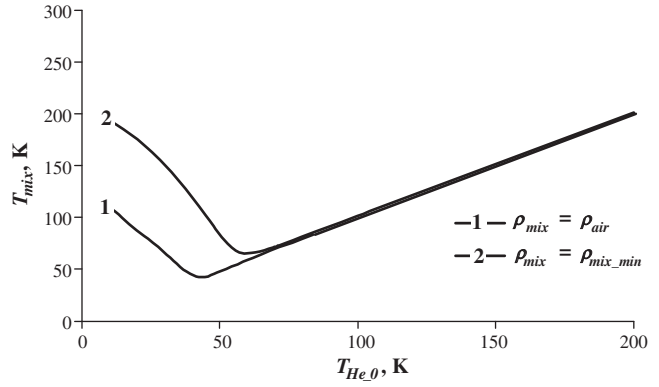

Fig. 7. Mixture temperature in the buoyant region.

decrease below the density of the air. We consider the equalization of the mixture and air density a necessary condition for the helium-rich layer stratification. We presume that the stratified layer density will stay between $\rho_{mix} = \rho_{air}$ and $\rho_{mix} = \rho_{mix\_min}$. Corresponding oxygen concentrations and mixture temperatures are shown in Figs. 6 and 7 as a function of the helium temperature at the relief point.

However, it is not possible to decide upon the parameters of the stratified layer, basing only on the above considerations, as the results calculated for $\rho_{mix} = \rho_{air}$ and $\rho_{mix} = \rho_{mix\_min}$ are significantly different from each other, if the discharged helium initial temperature is lower than 100 K for oxygen concentration, and 65 K for mixture temperature.

We derive a criterion for the onset of stratification and stratified flows categorization from dimensional analysis. We assume that a stratified flow of a helium–air mixture can be described by a function of the following dimensional arguments: tunnel diameter $D$, ventilation air velocity $u_{air}$, air density $\rho_{air}$, discharged helium mass flow rate $q_{m\_He}$,

initial helium density $\rho_{He}$, density difference between air and helium–air mixture $\Delta\rho$ and acceleration of gravity $g$.

$$f(D, u_{air}, \rho_{air}, q_{m\_He}, \rho_{He}, \Delta\rho, g) = 0 \quad (9)$$

Buckingham theorem leads to the following dimensionless equation:

$$F(\pi_1, \pi_2, \pi_3, \pi_4) = F\left(\frac{q_{m\_He}}{D^2 u_{air}\rho_{air}}, \frac{\rho_{He}}{\rho_{air}}, \frac{\Delta\rho}{\rho_{air}}, \frac{gD}{u_{air}^2}\right) = 0 \quad (10)$$

The combination of $\pi_1$, $\pi_2$, $\pi_3$ and $\pi_4$ described by Eq. (11) is similar to the Bakke number ($Ba$) used in the analysis of local methane accumulation in the mines and it is called here $Ba'$ [17].

$$\frac{\pi_2}{\pi_1\pi_3\pi_4} = \frac{u_{air}^3 \cdot D \cdot \rho_{air} \cdot \rho_{He}}{\Delta\rho \cdot q_{m\_He} \cdot g} = \frac{u_{air}}{\sqrt[3]{\frac{\Delta\rho \cdot q_{m\_He} \cdot g}{D \cdot \rho_{air} \cdot \rho_{He}}}} = Ba' \quad (11)$$

We notice that $Ba'$ dimensionless number can be also derived from a combination of Reynolds and Archimedes numbers:

$$(Ba')^3 = \frac{Re^2}{Ar} \cdot \frac{u_{air}}{u_{He}} \quad \text{and} \quad Re = \frac{u_{air}D}{\nu_{air}} \sim \frac{F_i}{F_\nu},$$
$$Ar = \frac{gD^3}{\nu_{air}^2}\frac{\Delta\rho}{\rho_{air}} \sim \frac{F_b}{F_\nu} \quad (12)$$

We propose a dimensionless number $Ba'$ as a criterion enabling the categorization of stratified flows of the helium–air mixture.

## 4. Experiment investigation of helium–air mixture stratification and propagation along a laboratory tunnel

A dedicated experiment was planned, aimed at the verification of stratified flow formation in a test tunnel, visualization and classification of helium–air mixtures flows, measurement of oxygen concentration and temperature profiles in the helium–air mixtures.

A scheme of the test-rig is presented in Fig. 8. The main part of the rig is a tunnel of an inner diameter 0.292 m and length 8.89 m, partially made of transparent plexi-glass to enable flow visualization. The tunnel slope is adjustable with a tolerance of ±2.8%.

Liquid helium was supplied from a pressurized 25 dm$^3$ Dewar vessel, through the vacuum insulated transfer line terminated with a regulated heater and a nozzle of an adjustable diameter. Helium at the required temperature was vented through the nozzle perpendicular to the tunnel pipe. The entrainment of air did not depend on the nozzle orientation which could have been changed even to horizontal position without influencing the stratified layer parameters. This observation corresponds to the conclusions derived from dimensional analysis, where the characteristic $Ba'$ number depends on the helium mass flow rate and the helium velocity. The Dewar vessel was placed on an electronic balance, which was used to determine the helium mass decrement and thus indirectly the helium mass flow rate.

The axial-flow fan with the speed regulator, of the maximal capacity equal to 0.63 m$^3$/s, was installed in order to force air flow in the tunnel. In order to obtain a uniform turbulent air velocity profile in the measurement zone, two flow straighteners (of 0.2 m length and 0.292 m diameter) packed with pipes of the diameter 0.016 m, the air reservoir (of 2 m high and 1.2 m diameter) and the converging cone were installed in the test set-up. Exemplary measured air velocity profiles are shown in Fig. 9.

The module with a set of sensors contains 10 oxygen sensors based on the limiting current method using zirconium solid electrolyte and 12 copper-constantan thermocouples. The oxygen sensors were individually calibrated to avoid discrepancies described by Arenius et al. [9]. The oxygen concentration and temperature were measured at distances of 5 $D$ and 10 $D$ down the helium flow and 5.5 $D$ up the flow. The helium outlet temperature was regulated with a Lake Shore temperature controller Model 331. The following parameters were monitored during the measurements: ambient temperature (average 292.5 K), pressure (average 1000 hPa), humidity (average 55%) and over-pressure in the Dewar vessel (0.2 MPa). During the experiments the helium mass flow rate was equal to 1 and 3 g/s, air velocity was within the range 0–2 m/s. The plan

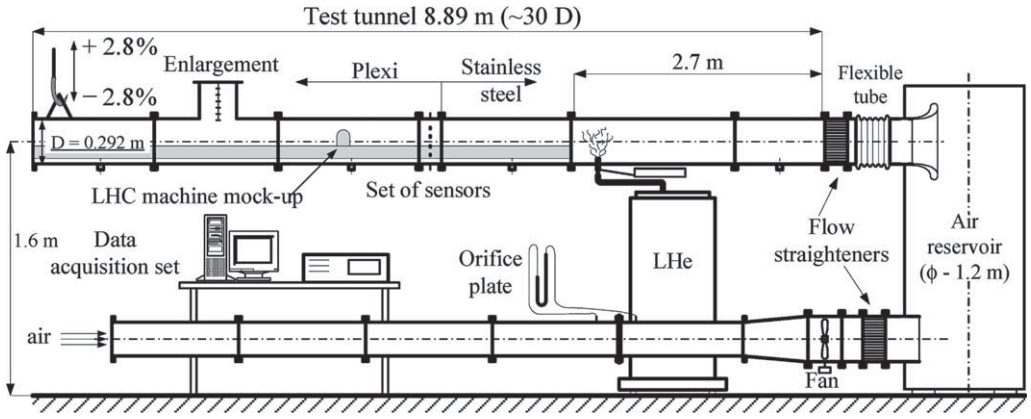


Fig. 8. Test set-up.

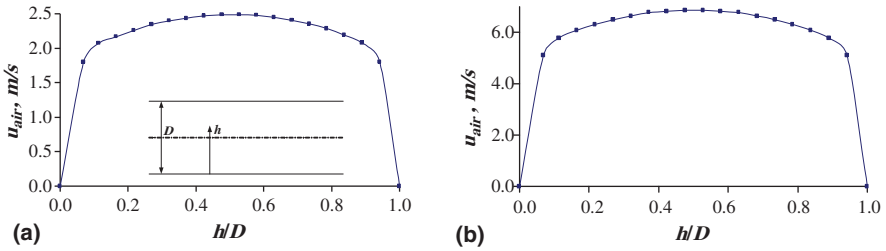


Fig. 9. Air velocity profiles measured in the test tunnel, at a distance 5 $D$ from the nozzle; (a) average velocity 2.27 m/s; (b) average velocity 6.31 m/s.

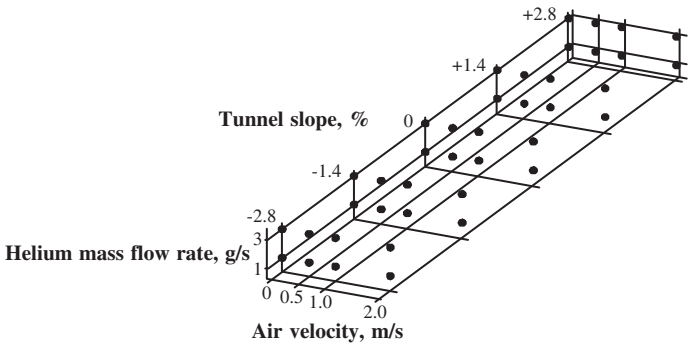


Fig. 10. Plan of the measurements.

of the performed experiments is shown in Fig. 10 where each dot denotes the parameters of one measurement series. The variation of $Ba'$ number was in the range from 0 to 10.

## 5. Helium–air mixture flow visualization

The flow visualization was based on the visibility of the condensed moisture in the helium-rich layer. The moisture was visible only when the mixture temperature dropped below the dew point. It is a general rule that the presence of mixture indicates the possible oxygen deficiency, while the lack of moisture does not guarantee the helium absence. We have identified five types of the helium–air mixture flow on the basis of the character of the visible moisture propagation along the test tunnel. The corresponding ranges of dimensionless $Ba'$ number were estimated experimentally. A summary of the visualization results is given in Fig. 11.

A fully stratified flow denoted as Type 1 was observed for the $Ba'$ number: $0 \leqslant Ba' < 2$, especially when the forced airflow was absent ($u_{air} = 0$, $Ba' = 0$). The mist was visible in the upper part of the tunnel as a layer of a practically constant thickness if the helium mass flow rate remained unchanged. The thickness of the layer was dependent on the initial helium mass flow rate. For $q_{m\_He} = 3$ g/s the layer was about one and a half times thicker than for $q_{m\_He} = 1$ g/s. The flow became unstable only when the air velocity increased above 0.3 m/s which corresponded to $Ba' \approx 2$.

Type 2 of the mixture flow was observed for $2 \leqslant Ba' < 4$, helium mass flow rates $q_{m\_He} = 3$ g/s and air velocity $u_{air} = 0.5$ m/s. In this case a dense mist was observed in the lower and central part of the test tunnel up to the level of 0.8–0.9 $D$.

Type 3 was characteristic for $4 \leqslant Ba' < 8$. A visible trail of the mist was located in the middle of the tunnel. This flow type was typical for a relatively lower helium mass flow rate ($q_{m\_He} = 1$ g/s) and low air velocity ($u_{air} = 0.5$ m/s) or higher helium mass flow rate ($q_{m\_He} = 3$ g/s) and intermediate air velocity ($u_{air} = 1.0$ m/s).

Type 4 is characteristic for $Ba' > 8$. In this type, close to the helium discharge point, at a distance of 5–7 $D$, the mist spread at the bottom of the tunnel, to raise further and move chaotically filling almost the whole tunnel cross-section. When the ratio $q_{m\_air}/q_{m\_He}$ exceeded 70, the distance of the tunnel with the mist at the lower part significantly shortened to 1–3 $D$ which made us to distinguish additionally Type 5 of the analyzed flow.

## 6. Oxygen concentration and temperature profiles for identified flow types

The oxygen concentration and the temperature profile measurements are shown in Fig. 12 and the summary of the measurements is given in Table 2. Each point represents a mean value of 100 readouts for temperature, and 150 readouts for oxygen concentration. It allowed statistical data handling and hence the assessment of the measurement accuracy. It has been assumed that the measurement results comply with the normal distribution, with the confidence level equal to 95%. Probability areas have been marked on the diagrams. The measurements were started 10 min after the initiation of helium discharge, when the

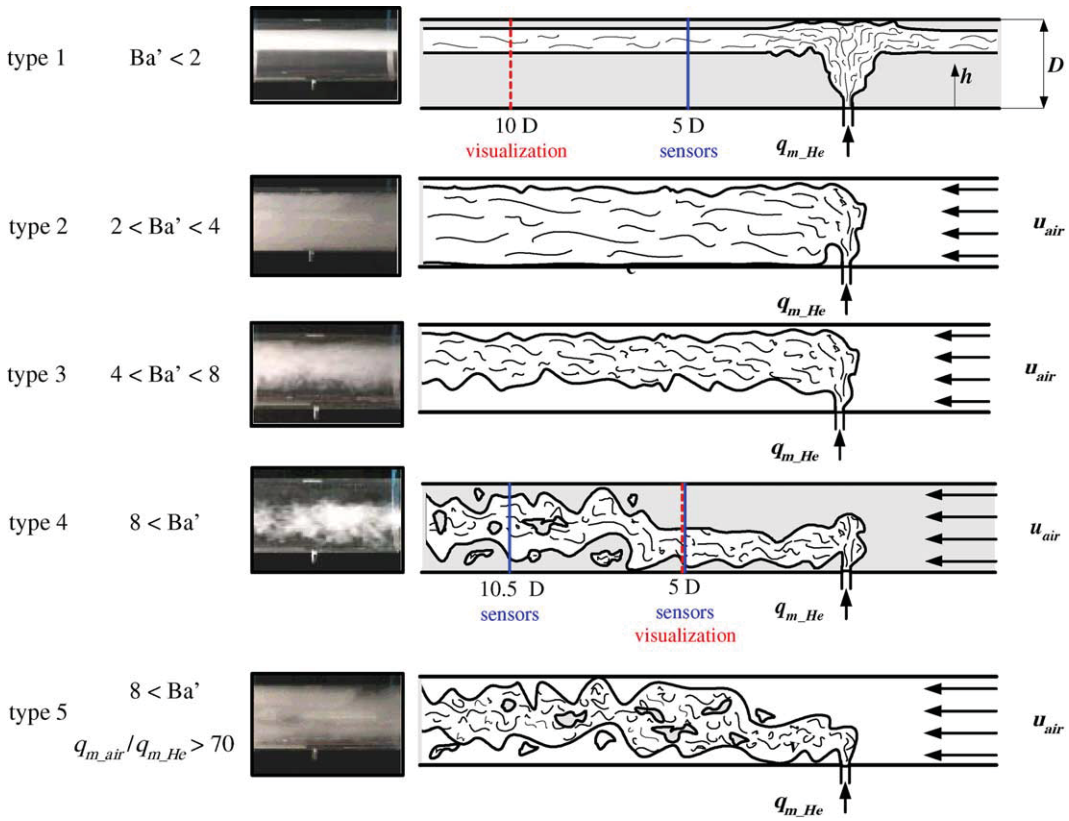


Fig. 11. Types of observed helium–air mixture flow patterns, tunnel slope 0%.

test rig temperature at a distance of 5 $D$ from the helium discharge point had stabilized.

The highest oxygen deficiency and the lowest helium–air mixture temperature were observed for the flow of type 1. The oxygen concentration decreased to 2–6% at the tunnel height of 0.5–1 $h/D$ for $q_{m\_He} = 1$ g/s and to 2–4% at the height of 0.4–1 $h/D$ for a higher helium mass flow rate ($q_{m\_He} = 3$ g/s). The temperature decreased to the value of about 230 K at 0.7 $h/D$ for $q_{m\_He} = 1$ g/s and to 190 K at 0.55 $h/D$ for $q_{m\_He} = 3$ g/s. Below the visible helium-rich layer, at the tunnel level of 0–0.2 $h/D$, the oxygen concentration remained at the level of 20%. It should be noticed that in the case of type 1 flow, the areas of visible mist presence corresponded with the levels of both the lowest oxygen concentration and the mixture temperature. The measurements of oxygen concentration in the stratified layer in the case of type 1 flow, made it possible to positively verify our assumption that the concentration of oxygen in this layer can be calculated using the one dimensional turbulent jet model. The measured oxygen content in the mixture corresponds to the condition $\rho_{mix} = \rho_{air}$, independently of the helium flow rate. The comparison of the measured and calculated mixture temperature reveals the discrepancies, as the calculated values are much lower than resulting from the experiment. The differences are the consequence of the fact that the model does not take into account the heat transfer between the mixture and tunnel wall.

In the case of type 2 flow, the oxygen concentration decreased of 7–9% in the upper and middle part of the tunnel (at the tunnel level of 0.3–0.9 $h/D$), while at the bottom (at the level of 0.3 $h/D$) the measured oxygen content was in the range of 10–15%. The lowest mixture temperature of ca. 240 K was measured in the middle of the tunnel (at 0.3–0.6 $h/D$).

For type 3 the oxygen concentration decrease to the values of 15–18% was registered at the level of 0.5–0.8 $h/D$ in the case of $q_{m\_He} = 1$ g/s and to values of 11–14% at 0.7–0.9 $h/D$, for $q_{m\_He} = 3$ g/s. It was followed by temperature decrease to 245–260 K at the upper part of the tunnel (0.7–0.9 $h/D$).

In the first zone of the flow type 4, when the mist spread at the bottom of the tunnel, a decrease to about 15% of oxygen concentration took place, at the level of 0.3 $h/D$. In the same region the temperature dropped to about 270 K at 0.2 $h/D$. In the second zone, at a distance higher than 7 $D$ from the helium discharge point, the oxygen concentration does not decrease below 20% up to the level 0.3 $h/D$, while above 0.3 $h/D$ it was measured at 16–18%. The temperature profile underwent flattening and the measured temperatures lay between 270 and 280 K.

Similar properties were observed in the case of type 5. The lowest oxygen content in the helium–air mixture was of about 18%. It was measured at the tunnel level of 0.8 $h/D$. The lowest measured temperature was about 270–280 K.

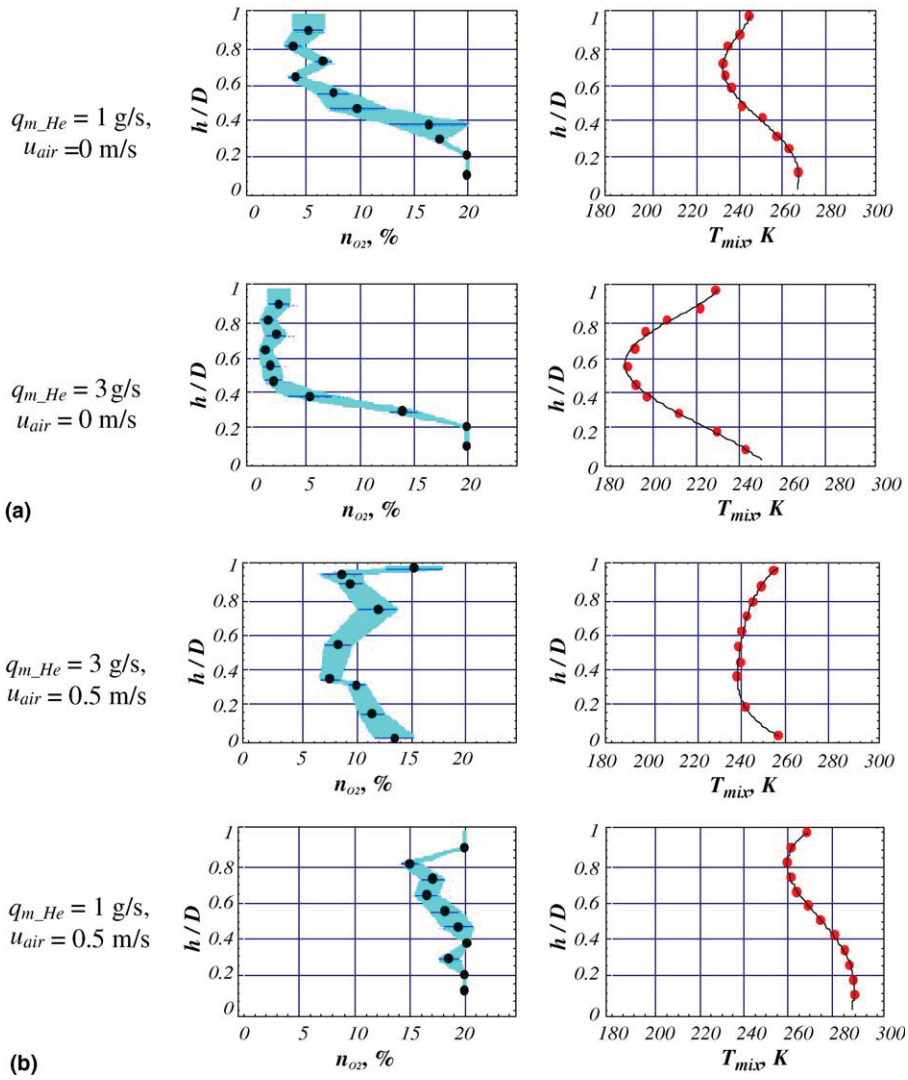


Fig. 12. Measured oxygen concentration and temperature profiles. (a) Type 1, (b) type 2, (c) type 3, (d) type 4, and (e) type 5.

It should be noticed that in the case of helium–air mixture flows qualified as types 2–5, the presence of visible mist does not necessary correspond to the region of the lowest oxygen content or highest temperature drop.

### 6.1. Safety aspects of identified flow types

However the lowest oxygen concentration was observed in case of a fully stratified flow (type 1, $Ba' < 2$), this flow type can be considered as the preferred from safety point of view. The oxygen concentration at the lower part of the tunnel remains practically unchanged at the safe level of above 18% and the oxygen deficient layer is clearly visible thanks to the condensed moisture, at least at the vicinity to the discharge point, as long as the mixture temperature remains below the dew point.

The most dangerous, and to be avoided from safety point of view, is the type 2 flow ($2 < Ba' < 4$). The oxygen concentration remains much below the safe value of 18% across a full cross-section of the tunnel. Oxygen concentration deficiencies in type 3 ($4 < Ba' < 8$) and type 4 flows are also important but not in life dangerous range of below 15%. Thus these flows should be avoided, if possible. Flow type 5 ($4 < Ba' < 8$, and $q_{m\_air}/q_{m\_He} > 70$), however demonstrating oxygen concentration decrease across the whole tunnel cross-section, is safe, as the content of oxygen nowhere drops below 18%. It is then recommended either to stay with the $Ba'$ number below 2, or to go above 8 and to keep $q_{m\_air}/q_{m\_He} > 70$.

## 7. Influence of the tunnel slope on the oxygen concentration and temperature drop

The test tunnel was set to positive and negative inclination angles of ±1.4% and ±2.8%.

Generally, it should be noticed that flow patterns and the shapes of the oxygen concentration and temperature profiles were not modified significantly. Only the location of the areas characterized by the lowest oxygen concentration and the lowest mixture temperature changed (see Figs.

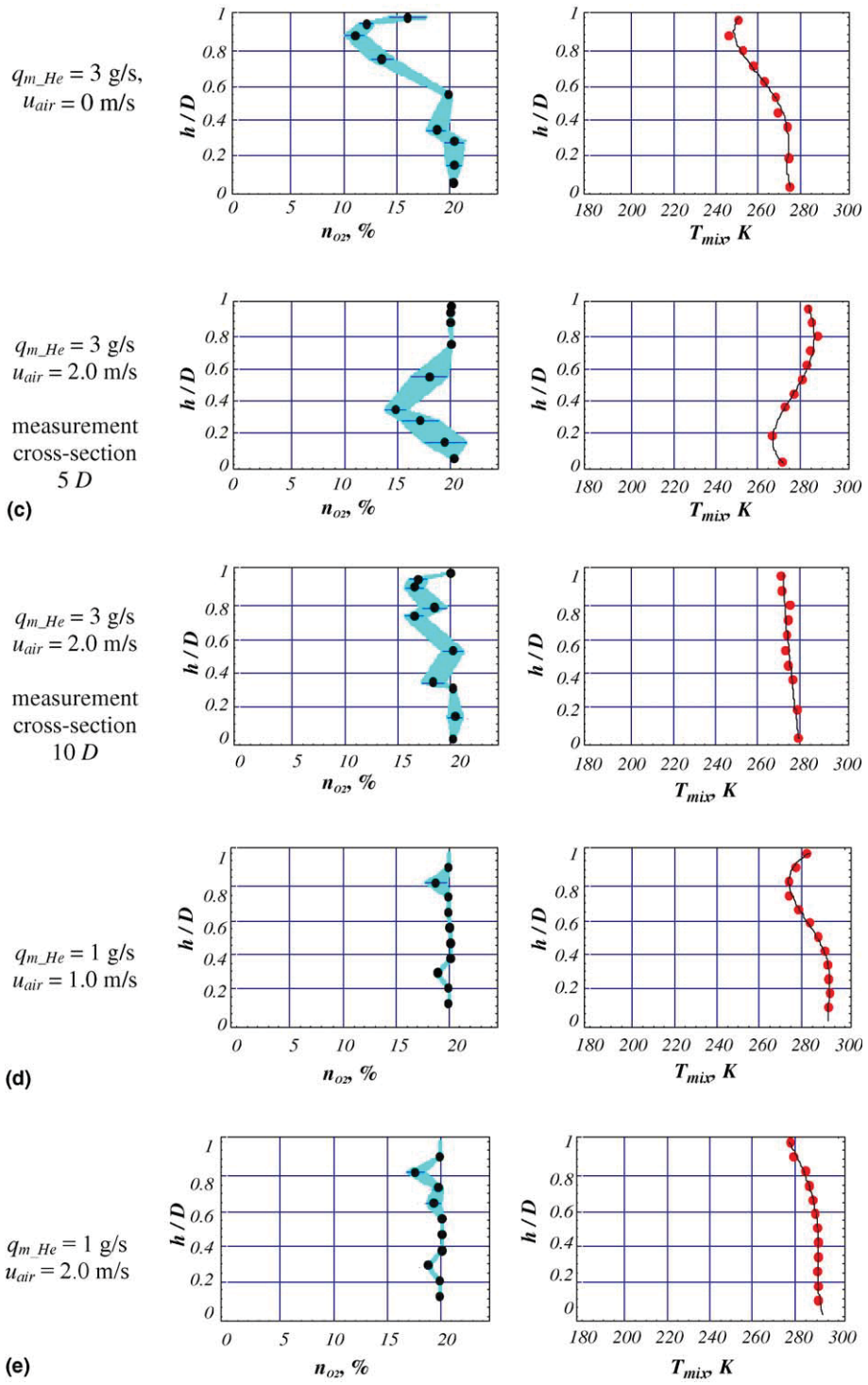


Fig. 12 (*continued*)

13 and 14). In the case of the tunnel slope equal to +2.8% areas of the highest oxygen deficiency (ca. 10% of oxygen content for $q_{m\_He} = 1$ g/s and ca. 7% for $q_{m\_He} = 3$ g/s) were observed from the level of 0.55 $h/D$ and 0.6 $h/D$, correspondingly, for helium mass flow rates equal to 1 and 3 g/s. In the case of the opposite inclination (tunnel slope −2.8%) the lowest oxygen concentration was located at the level of 0.4 $h/D$ for $q_{m\_He} = 1$ g/s and 0.3 $h/D$ for $q_{m\_He} = 3$ g/s. Also the composition of the stratified mixture changed. The oxygen concentration measured for the tunnel slope −2.8% was in the range between 5% and 6% in the case of $q_{m\_He} = 1$ g/s and about 2–4% for $q_{m\_He} = 3$ g/s. A similar property was revealed by the mixture temperature. While for slope +2.8% the lowest temperature of about 255 K was measured at the level of about 0.8 $h/D$ for both helium mass flow rates, the lowest

Table 2
Summary of experimental results

| Flow condition | Flow type | The lowest $n_{O_2}$ and its location | | The lowest $T_{mix}$ and its location | | $Ba'$ number |
|---|---|---|---|---|---|---|
| | | $n_{O_2}$,% | $h/D$ | $T_{mix}$ (K) | $h/D$ | |
| $q_{m\_He} = 1$ g/s, $u_{air} = 0$ m/s | 1 | 2–6 | 0.5–1 | 230 | 0.7 | $Ba' < 2$ |
| $q_{m\_He} = 1$ g/s, $u_{air} = 0.5$ m/s | 3 | 15–18 | 0.5–0.8 | 260 | 0.8 | $4 < Ba' < 8$ |
| $q_{m\_He} = 1$ g/s, $u_{air} = 1.0$ m/s | 5 | 18 | 0.8 | 270 | 0.8 | $8 < Ba'$ |
| $q_{m\_He} = 1$ g/s, $u_{air} = 2.0$ m/s | | | | 280 | 0.9 | |
| $q_{m\_He} = 3$ g/s, $u_{air} = 0$ m/s | 1 | 2–4 | 0.4–1 | 190 | 0.55 | $Ba' < 2$ |
| $q_{m\_He} = 3$ g/s, $u_{air} = 0.5$ m/s | 2 | 7–9 | 0.3–0.9 | 240 | 0.3–0.6 | $2 < Ba' < 4$ |
| $q_{m\_He} = 3$ g/s, $u_{air} = 1.0$ m/s | 3 | 11–14 | 0.7–0.9 | 245 | 0.85 | $4 < Ba' < 8$ |
| $q_{m\_He} = 3$ g/s, $u_{air} = 2.0$ m/s | 4 | 15 | 0.3 | 270 | 0.2 | $8 < Ba'$ |

temperatures for slope of −2.8% were measured at 0.45 $h/D$ and 0.4 $h/D$, correspondingly, for $q_{m\_He} = 1$ g/s (ca. 260 K) and $q_{m\_He} = 3$ g/s (ca. 245 K).

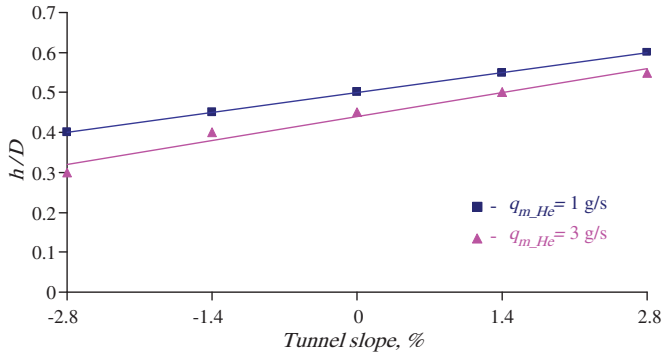


Fig. 13. Influence of the test tunnel slope on the position of the lowest oxygen concentration areas in case of stratified flow.

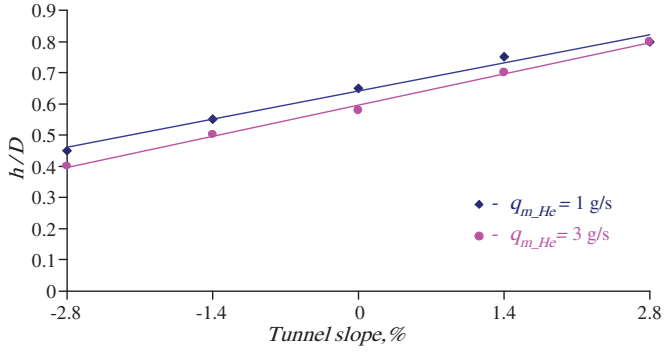


Fig. 14. Influence of the test tunnel slope on the position of the lowest mixture temperature point in case of stratified flow.

## 8. Influence of air velocity

It should be noticed that along with the air velocity increasing, both oxygen concentration and mixture temperature profiles showed the tendency to flatten and to become uniform as a result of more intensive and homogenous mixing of mixture components. Only the first zone of flow type 4 made an exception. In this case the mixture spread in the ground part of the tunnel. But at a distance bigger than 7 $D$ the mixture became practically homogenous in the whole tunnel cross-section (compare Fig. 12).

## 9. Case study—safety analysis in the LHC tunnel

The presented approach has been used to analyse the oxygen deficiency hazard consequences expected in result of potential failures of supply header C of the LHC cryogenic distribution line. The estimated helium flow and discharge temperature are given in Table 3. First the properties of the helium–air mixture resulting from discharged helium parameters [1] and the turbulent jet mechanism have been estimated (see Table 3). The available length of the helium jet formation in the LHC tunnel is of about 1.5 m (see Fig. 5). At this distance buoyant conditions can be reached and stratification of the helium-rich mixture observed. Then, taking into account air velocities in the LHC tunnel resulting form the ventilation conditions, the flow patterns depending on the $Ba'$ number have been determined (see Table 4). In case of air flow velocity equal to 0.55 m/s stratified flow of type 1 is expected, while in case of the air velocity of 0.88 m/s the flow will be of type 1 or 2.

Table 3
Helium–air mixture properties following potential emergency helium discharge from the LHC cryogenic system

| Conditions at the helium outlet | Characteristic jet cross-sections | $x$ (m) | $\rho_{mix}$ (kg/m$^3$) | $T$ (K) | $n_{O_2}$ (%) |
|---|---|---|---|---|---|
| $q_{m\_He} = 3$ kg/s, $T_{He\_0} = 25$ K | $\rho_{mix} = \rho_{air}$ | 0.41 | 1.20 | 75 | 2.6 |
| | $\rho_{mix} = \rho_{min}$ | 1.32 | 1.08 | 164 | 8.5 |
| | $x = 1.2$ m | 1.20 | 1.09 | 156 | 8.0 |
| $q_{m\_He} = 1$ kg/s, $T_{He\_0} = 20$ K | $\rho_{mix} = \rho_{air}$ | 0.54 | 1.20 | 87 | 3.5 |
| | $\rho_{mix} = \rho_{min}$ | 1.67 | 1.09 | 174 | 9.4 |
| | $x = 1.2$ m | 1.20 | 1.10 | 147 | 7.4 |

Table 4
Dimensionless $Ba'$ numbers and flow types estimated for potential emergency helium discharge from the LHC cryogenic system

| Conditions at the helium outlet | $Ba'$ | | Flow type | |
|---|---|---|---|---|
| | $u_{air} = 0.55$ m/s | $u_{air} = 0.88$ m/s | $u_{air} = 0.55$ m/s | $u_{air} = 0.88$ m/s |
| $q_{m\_He} = 3$ kg/s, $T_{He\_0} = 25$ K | 0.76 | 1.64 | Type 1 | Type 1 |
| $q_{m\_He} = 1$ kg/s, $T_{He\_0} = 20$ K | 1.22 | 2.65 | Type 1 | Type 2 |

## 10. Conclusions

In case of emergency relief of the helium filling cryogenic installations of superconducting accelerators, oxygen deficiency hazard arises. Safe operation of the installations requires good understanding of the air–helium mixture origin process, allowing the estimation of the maximum depletion of oxygen content in the atmosphere. The location of oxygen deficient mixture, its potential separation and propagation along the tunnel should also be recognized.

The paper proposes a description of helium–air mixture formation based on turbulent jet physics. The approach allows the estimation of the helium–air mixture properties, like temperature and oxygen concentration, especially significant in safety analysis. It has been concluded and experimentally validated that for the helium discharge temperature lower than 45 K, the condition $\rho_{mix} = \rho_{air}$ is sufficient to obtain a separated helium–air mixture. The calculated oxygen content in the mixture remains in good agreement with experimental results. The estimation accuracy is sufficient for the safety oxygen deficiency hazard analysis.

Potential stratification of the helium–air mixture can be predicted on the basis of dimensionless $Ba'$ number. This number decides also on the type of the stratified flow in the tunnel.

To keep a breathable atmosphere at least at lower part of the tunnel cross-section, a stratified flow characterised by $Ba' < 2$ is desirable. The other safe possibility is a fully homogenous flow characterised by $4 < Ba' < 8$, and $q_{m\_air}/q_{m\_He} > 70$.

## Acknowledgements

The study was executed in the framework of the collaboration agreement between CERN, Geneva and Wroclaw University of Technology, Poland.

## References

[1] Chorowski M, Lebrun Ph, Riddone G. Preliminary risk analysis of the LHC cryogenic system. Advances in cryogenic engineering 45B. New York: Plenum; 2000. p. 1309–16.
[2] Edeskuty FJ, Stewart WF. Safety in the handling of cryogenic fluids. New York: Plenum Press; 1996.
[3] Jia LX, Wang L. Equations for gas releasing process from pressurised vessel in ODH evaluation. Advances in cryogenic engineering 47B. New York: Melville; 2002. p. 1792–8.
[4] Soyars WM, Schiller JL. Open channel helium flow during rapture event. Advances in cryogenic engineering 47B. New York: Melville; 2002. p. 1776–83.
[5] Chorowski M, Konopka G, Riddone G. An experimental study of cold helium dispersion in air. Advances in cryogenic engineering 47B. New York: Melville; 2002. p. 1452–9.
[6] Chorowski M, Konopka G, Riddone G, Rybkowski D. Experimental simulation of helium discharge into the LHC tunnel. Proceedings of the nineteenth international cryogenic engineering conference. New Delhi: Narosa Publishing House; 2003. p. 67–70.
[7] Horlitz G. Einige Folgen grosser Leckes im Heliumsystem des supraleitened Magnetsystem von HERA, ihre Auswirkungen auf die Tunnelatmosphaere und Konsequenzen fur den Personenchutz. DESY HERA 81/13, September 1981.
[8] Casebolt H, Limon J. Simulation of accident involving the release of liquid helium into the main ring tunnel. Courtesy of Thomas Jefferson National Accelerator Facility, USA; 1999.
[9] Arenius D, Curry D, Hutton A, Mohoney K, Prior S, Robertson H. Investigation of personal and fixed head oxygen deficiency hazard monitoring performance for helium gas. Advances in cryogenic engineering: proceedings of the cryogenic engineering conference, vol. 47. New York: Melville; 2002. p. 1784–91.
[10] Berg H, Clausen M, Herzog H, Horlitz G, Lierl H. Report on operational experience and reliability of the HERA cryogenic system. Advance in cryogenic engineering: proceedings of the cryogenic engineering conference, vol. 39. New York: Plenum Press; 1994. p. 571–9.
[11] Peterson T. Helium and nitrogen ODH analysis for ICB Engineering Laboratory. Fermilab. Courtesy of Fermi National Accelerator Laboratory, USA; 1991.
[12] Rode CH, Chronis WC, Keesee M, Ahlaman D, Brazzale D, Hansknecht J, et al. Injector helium spill test. Courtesy of Thomas Jefferson National Accelerator Facility, USA; 1991.
[13] Mahoney K, Hutton A, Robertson H, Arenius D, Curry D. Helium sensitivity in oxygen deficiency measurement equipment. Courtesy of Thomas Jefferson National Accelerator Facility, USA; 2001.
[14] Landau LD, Lifszyc EM. Hydrodynamics. Warsaw: WNT PWN; 1994.
[15] Chorowski M. Combined thermo-hydraulic analysis of a cryogenic jet. Advances in cryogenic engineering: proceedings of the cryogenic engineering conference, vol. 45. New York: Plenum Press; 2000. p. 1189–96.
[16] Konopka-Cupial G. Investigation of helium–air mixture flows. Ph.D. thesis, Report 04/2004. Wroclaw University of Technology, Institute of Heat Engineering and Fluid Mechanics, Wroclaw, 2004 [in Polish].
[17] Struminski A, Suchodolski Z. Ventilation of mine threaten by rock explosion and gas discharge. Wroclaw: Wydawnictwo Politechniki Wroclawskiej; 1993 [in Polish].